

## Colloid Movement in Unsaturated Porous Media: Recent Advances and Future Directions

Nicole M. DeNovio, James E. Saiers, and Joseph N. Ryan\*

### ABSTRACT

Investigations of colloid movement through geologic materials are driven by a variety of issues, including contaminant transport, soil-profile development, and subsurface migration of pathogenic microorganisms. In this review, we address recent advances in understanding of colloid transport through partially saturated porous media. Special emphasis is placed on features of the vadose zone (i.e., the presence of air–water interfaces, rapid fluctuations in porewater flow rates and chemistry) that distinguish colloid transport in unsaturated media from colloid transport in saturated media. We examine experimental studies on colloid deposition and mobilization and survey recent developments in modeling colloid transport and mass transfer. We conclude with an overview of directions for future research in this field.

**M**OBILE COLLOIDS are ubiquitous in the porewaters of vadose zone soils. Concentrations in excess of  $1 \text{ g L}^{-1}$  have been reported during simulated and natural rainfall events (Table 1). The colloids include mineral fragments, microbes, and plant decay debris, with mineral fragments being the most plentiful in typical soils. The mineral fragments are derived mainly from the soil itself, which contains a great abundance of particles in the colloidal size range (Wu et al., 1993; Grout et al., 1998; Posadas et al., 2001). The colloidal size range is about 10 nm to 10  $\mu\text{m}$ , with the smallest colloids being those that are just larger than dissolved macromolecules, and the largest colloids being those that resist settling once suspended in soil porewaters.

Colloid movement in the vadose zone is of concern for four major reasons:

1. The movement of mobile colloids may facilitate the transport of some contaminants (Amrhein et al., 1993; de Jonge et al., 1998; Ryan et al., 1998; McGechan and Lewis, 2002).
2. The movement of pathogenic microbes (“biocolloids”) during wastewater reclamation and aquifer recharge presents a public health risk (Hurst, 1980; Powelson et al., 1993; Redman et al., 2001).
3. The deposition of mobile colloids may reduce soil permeability (Quirk and Schofield, 1955; Frenkel et al., 1978; Baveye et al., 1998).
4. The movement of colloids through the vadose zone (illuviation) is an important process in soil genesis

(Buol and Hole, 1961; McKeague and St. Arnaud, 1969; Matlack and Houseknecht, 1989).

How do these colloids become suspended in porewater? Are they readily transported through the vadose zone? How rapidly are these colloids deposited back onto soil surfaces? These questions can be addressed, in part, by examining processes of colloid deposition and mobilization in saturated porous media (McDowell-Boyer et al., 1986; Ryan and Elimelech, 1996), but in this review, we focus on what is known about these processes in unsaturated porous media.

Three key features of the vadose zone play a critical role in colloid movement: (i) the presence of air–water interfaces, (ii) transients in flow and chemistry, and (iii) soil structure and heterogeneity (Fig. 1). First, the unsaturated nature of the vadose zone introduces a third phase, air, which affects colloid partitioning between water and soil. Colloids of many types associate with the air–water interface (Wan and Wilson, 1994b; Sirivithayapakorn and Keller, 2003), and the movement of these colloids is affected by the movement of air bubbles (Gomez-Suarez et al., 1999; Gomez-Suarez et al., 2001; Saiers et al., 2003). Second, porewater flow and chemistry are highly transient in unsaturated porous media. Flow transients, generated by rainfall and snowmelt events interspersed by drying periods, can promote very rapid colloid mobilization (El-Farhan et al., 2000). Chemical transients, often produced by the introduction of low ionic-strength rainwater into the vadose zone, result in destabilization of colloidal aggregates in soils and mobilization of colloids (e.g., Kaplan et al., 1993; Ryan et al., 1998). Third, the soils of the vadose zone are usually structured or physically heterogeneous to some extent. For example, macropores promote preferential flow that has the potential to augment colloid mobilization and reduce colloid deposition. Soil layering often inhibits colloid movement by enhancing deposition of colloids mobilized in the upper soil horizons (Bond, 1986).

In this review, we emphasize processes that control the transfer of inorganic colloids between immobile phases of unsaturated porous media and moving porewater. Microbes and particulate organic matter are not considered in detail, nor are the effects of solution composition, soil composition, biota, and soil aggregate structure on the dispersion and stability of soil colloids. These factors have been studied extensively (e.g., Renegasamy et al., 1984; Pojasok and Kay, 1990; Brubaker et al., 1992; Oades, 1993; Le Bissonnais, 1996), but usually in batch systems that do not elucidate the mass-transfer processes that occur during flow. We begin by examining colloid deposition and mobilization in “ideal” soils, or unsaturated porous media composed of grains of uniform size and shape (Table 2), and survey the

N.M. DeNovio and J.N. Ryan, Department of Civil, Environmental, and Architectural Engineering, University of Colorado at Boulder, 428 UCB, Boulder, CO 80309-0428; J.E. Saiers, School of Forestry and Environmental Studies, Yale Univ., Sage Hall, 205 Prospect Street, New Haven, CT 06511. Received 22 Jan. 2004. Special Section: Colloids and Colloid-Facilitated Transport of Contaminants in Soils. \*Corresponding author (joseph.ryan@colorado.edu).

Published in Vadose Zone Journal 3:338–351 (2004).  
© Soil Science Society of America  
677 S. Segoe Rd., Madison, WI 53711 USA

**Table 1.** Examples of studies on colloid mobilization, deposition, and transport in natural soils during simulated rainfall in laboratory columns and in field experiments. The following variables are used in characterization of the experiments: volumetric discharge ( $Q$ ), specific discharge ( $q$ ), influent colloid concentration ( $C$ ), ionic strength ( $I$ ), moisture content ( $\theta$ ), specific conductance (SC), isoelectric point ( $pH_{\text{iep}}$ ), electrophoretic mobility (EM), and zeta potential ( $\zeta$ ).

Reference	Porous medium	Water chemistry	Water flow	Colloid nature	Colloid concentration mg L <sup>-1</sup>	Major results
Pilgrim and Huff (1983)	<ul style="list-style-type: none"> <li>in situ field experiment</li> <li>Gaviota loam, Allamont clay loam</li> <li>macroporous</li> <li><math>3 \times 3 \times 1.5</math> m tank packed with soil</li> <li>Blanton sand (Ap and E horizons)</li> </ul>	<ul style="list-style-type: none"> <li>natural rainfall</li> <li>tap water</li> <li>SC = 6 <math>\mu\text{S cm}^{-1}</math></li> <li>pH 6.1</li> </ul>	<ul style="list-style-type: none"> <li>two rainfall events (<math>q</math>, 25 mm)</li> <li>irrigation sprinklers (<math>q = 10.7</math> mm h<sup>-1</sup>)</li> <li>rain simulator</li> <li><math>q = 5.1</math> cm h<sup>-1</sup></li> <li>duration 2 h</li> </ul>	<ul style="list-style-type: none"> <li>natural colloids</li> <li>size 4–8 <math>\mu\text{m}</math></li> <li>organic fraction 10%</li> <li>natural colloids: kaolinite, quartz, vermiculite, gibbsite, ferric oxides</li> <li>size 0.24–0.42 <math>\mu\text{m}</math></li> <li>EM = -2.4 to -3.4 <math>\mu\text{m s}^{-1}</math> cm V<sup>-1</sup></li> <li>natural colloids: illite, kaolinite, vermiculite</li> </ul>	100–5300	<ul style="list-style-type: none"> <li>colloid concentration increased with time during rainfall</li> <li>macropores allowed transport of larger colloids</li> <li>colloid concentration and size increased with increasing flow rate</li> <li>EM decreased with increasing flow rate</li> <li>clay mineral content increased and metal oxide content decreased with increase in flow rate</li> </ul>
Biddle et al. (1995)	<ul style="list-style-type: none"> <li>in situ field experiment</li> <li>two soils: Aquic Haploxeralf, Mollic Endoaqualf</li> </ul>	<ul style="list-style-type: none"> <li>natural rainfall</li> </ul>	<ul style="list-style-type: none"> <li>two natural rainfall events of same duration and intensity</li> <li>rain simulator</li> <li><math>q = 11</math> and 30 mm h<sup>-1</sup></li> <li>no ponding</li> </ul>	<ul style="list-style-type: none"> <li>illite: 46% &lt;2 <math>\mu\text{m}</math>, <math>\zeta = -13</math> mV</li> <li>illite/Aldrich humic acid: 27% &lt;2 <math>\mu\text{m}</math>, <math>\zeta = -17</math> mV</li> <li>natural colloids: kaolinite, ferric oxides, gibbsite, quartz, vermiculite</li> <li>size <math>\leq 1</math> <math>\mu\text{m}</math></li> <li>organic matter 1%</li> </ul>	13–290	<ul style="list-style-type: none"> <li>favorable assessment of capillary wick lysimeters for soil collection</li> </ul>
Jacobsen et al. (1997)	<ul style="list-style-type: none"> <li>intact cores in laboratory columns</li> <li>sandy loam (moraine deposit); Typic Hapludalf</li> <li>macroporous</li> </ul>	<ul style="list-style-type: none"> <li>tap water</li> <li>SC = 300 <math>\mu\text{S cm}^{-1}</math></li> <li>pH 7.0</li> </ul>	<ul style="list-style-type: none"> <li>rain simulator</li> <li><math>q = 11</math> and 30 mm h<sup>-1</sup></li> <li>no ponding</li> <li>natural rainfall</li> </ul>	<ul style="list-style-type: none"> <li>illite: 46% &lt;2 <math>\mu\text{m}</math>, <math>\zeta = -13</math> mV</li> <li>illite/Aldrich humic acid: 27% &lt;2 <math>\mu\text{m}</math>, <math>\zeta = -17</math> mV</li> <li>natural colloids: kaolinite, ferric oxides, gibbsite, quartz, vermiculite</li> <li>size <math>\leq 1</math> <math>\mu\text{m}</math></li> <li>organic matter 1%</li> </ul>	20–550	<ul style="list-style-type: none"> <li>particle size in effluent decreased with time</li> <li>greater mass recovery was observed at higher rainfall rate</li> <li>no significant difference was observed in the transport of humic acid-coated illite and uncoated illite</li> <li>colloid size decreased with time</li> <li>colloid mass increased with square root of time (suggesting diffusion-controlled kinetics of mobilization)</li> <li>colloid surface charge was highly negative</li> <li>colloids originated from surface horizons</li> <li>smaller colloids more abundant</li> <li>kaolinite, ferric oxide, gibbsite were enriched in smaller colloids</li> <li>larger particles were preferentially removed during transport</li> </ul>
Kaplan et al. (1997)	<ul style="list-style-type: none"> <li><math>3 \times 3 \times 1.5</math> m tank packed with soil</li> <li>Ultisol</li> </ul>	<ul style="list-style-type: none"> <li>natural rainfall</li> </ul>	<ul style="list-style-type: none"> <li>natural rainfall</li> </ul>	<ul style="list-style-type: none"> <li>natural colloids: kaolinite, montmorillonite, quartz, microcline, ferric oxyhydroxide</li> <li>size 1–20 <math>\mu\text{m}</math></li> <li><math>pH_{\text{iep}}</math> 3–4</li> <li>natural colloids</li> <li>organic C fraction 0.3–12%</li> </ul>	20–9800	<ul style="list-style-type: none"> <li>no correlation was observed between colloid concentration and flow velocity</li> <li>colloids mobilized decreased with successive rainfalls at 5–10 d intervals</li> <li>no change was observed in particle size with flow velocity</li> <li>no correlation was observed between colloids mobilized and soil grain size or composition</li> <li>colloid concentration increased with decrease in SC</li> <li>colloidal organic carbon decreased with time</li> <li>colloid mobilization rate increased with increase in outflow rate</li> <li>mass of mobilized colloids increased with the square root of time (suggesting diffusion-controlled mobilization kinetics)</li> </ul>
Ryan et al. (1998)	<ul style="list-style-type: none"> <li>loam, Aridic Argiustoll</li> <li>macroporous</li> <li>in situ field experiment</li> </ul>	<ul style="list-style-type: none"> <li>tap water</li> <li>SC = 30 <math>\mu\text{S cm}^{-1}</math></li> </ul>	<ul style="list-style-type: none"> <li>rain simulator</li> <li><math>q = 4.2</math>–16.7 cm h<sup>-1</sup></li> <li>duration 0.5–2 h</li> </ul>	<ul style="list-style-type: none"> <li>natural colloids: kaolinite, montmorillonite, quartz, microcline, ferric oxyhydroxide</li> <li>size 1–20 <math>\mu\text{m}</math></li> <li><math>pH_{\text{iep}}</math> 3–4</li> <li>natural colloids</li> <li>organic C fraction 0.3–12%</li> </ul>	20–9800	<ul style="list-style-type: none"> <li>no correlation was observed between colloid concentration and flow velocity</li> <li>colloids mobilized decreased with successive rainfalls at 5–10 d intervals</li> <li>no change was observed in particle size with flow velocity</li> <li>no correlation was observed between colloids mobilized and soil grain size or composition</li> <li>colloid concentration increased with decrease in SC</li> <li>colloidal organic carbon decreased with time</li> <li>colloid mobilization rate increased with increase in outflow rate</li> <li>mass of mobilized colloids increased with the square root of time (suggesting diffusion-controlled mobilization kinetics)</li> </ul>
Lægdsmand et al. (1999)	<ul style="list-style-type: none"> <li>intact cores in laboratory columns</li> <li>sandy loam, Alfisol, Typic Hapludalf</li> <li>macroporous</li> </ul>	<ul style="list-style-type: none"> <li>synthetic rain water</li> <li>SC 30 <math>\mu\text{S cm}^{-1}</math></li> <li>pH 4.6</li> </ul>	<ul style="list-style-type: none"> <li>rain simulator</li> <li><math>q = 1.6</math>–6.5 mm h<sup>-1</sup></li> </ul>	<ul style="list-style-type: none"> <li>natural colloids</li> <li>organic C fraction 0.3–12%</li> </ul>	3–45	<ul style="list-style-type: none"> <li>colloid concentration increased with decrease in SC</li> <li>colloidal organic carbon decreased with time</li> <li>colloid mobilization rate increased with increase in outflow rate</li> <li>mass of mobilized colloids increased with the square root of time (suggesting diffusion-controlled mobilization kinetics)</li> </ul>

Continued next page.

Table 1. Continued.

Reference	Porous medium	Water chemistry	Water flow	Colloid nature	Colloid concentration	Major results
El-Farhan et al. (2000)	<ul style="list-style-type: none"> <li>in situ field experiments</li> <li>Frederick, Lodi silt loam, Typic Hadtult</li> <li>highly structured</li> </ul>	<ul style="list-style-type: none"> <li>0.1 M NaCl solution</li> </ul>	<ul style="list-style-type: none"> <li>ponding</li> <li>5–20 cm initial depth</li> </ul>	<ul style="list-style-type: none"> <li>natural colloids</li> <li>size 253–270 nm</li> </ul>	<ul style="list-style-type: none"> <li>7–265 mg L<sup>-1</sup></li> </ul>	<ul style="list-style-type: none"> <li>mass of colloids mobilized decreased with successive infiltration events</li> <li>colloid mass flux was steady among infiltration events</li> <li>peak colloid concentrations and flux were observed during rising and falling limbs of water flux (suggesting moving air–water interfaces caused mobilization)</li> <li>colloid breakthrough increased with increase in moisture content</li> <li>colloid breakthrough increased with increase in abundance of larger pore sizes in porous medium</li> <li>colloid breakthrough increased with decrease in colloid size</li> <li>colloid surface charge and cation saturation had little effect on colloid breakthrough</li> <li>increased colloid breakthrough with decreased ionic strength</li> <li>increased colloid breakthrough with increased moisture content</li> </ul>
Noack et al. (2000)	<ul style="list-style-type: none"> <li>sieved fractions packed in laboratory column</li> <li>Oxisol, clay texture</li> <li>Spodosol, sandy clay texture</li> </ul>	<ul style="list-style-type: none"> <li>distilled water</li> <li>SC &lt; 10 μS cm<sup>-1</sup></li> <li>pH 5.5</li> </ul>	<ul style="list-style-type: none"> <li>rain simulator</li> <li>q = 50 mm h<sup>-1</sup></li> <li>θ = 0.28–0.59</li> </ul>	<ul style="list-style-type: none"> <li>Muloorina illite, size 0.07 μm</li> <li>Fifhian illite, two size fractions, 0.08–0.2, 1–2 μm</li> <li>soil fraction composed of illite, kaolinite, size 0.08–0.2 μm</li> </ul>	<ul style="list-style-type: none"> <li>C = 100</li> </ul>	<ul style="list-style-type: none"> <li>colloid breakthrough increased with increase in moisture content</li> <li>colloid breakthrough increased with increase in abundance of larger pore sizes in porous medium</li> <li>colloid breakthrough increased with decrease in colloid size</li> <li>colloid surface charge and cation saturation had little effect on colloid breakthrough</li> <li>increased colloid breakthrough with decreased ionic strength</li> <li>increased colloid breakthrough with increased moisture content</li> </ul>
Gamerding and Kaplan (2001)	<ul style="list-style-type: none"> <li>laboratory centrifuge column</li> <li>Yucca Mountain tuff (0.25–0.84 mm)</li> </ul>	<ul style="list-style-type: none"> <li>deionized water</li> <li>carbonate/bicarbonate solution</li> <li>I = 12 mM</li> <li>pH 7.8</li> <li>tap water</li> <li>SC = 22 μS cm<sup>-1</sup></li> <li>pH 7.8</li> </ul>	<ul style="list-style-type: none"> <li>flow driven by centrifugation</li> <li>θ = 0.06–0.19</li> </ul>	<ul style="list-style-type: none"> <li>polystyrene latex microspheres, size 280 nm, carboxyl-modified</li> </ul>	<ul style="list-style-type: none"> <li>C = 4.5</li> </ul>	<ul style="list-style-type: none"> <li>colloid mobilization dominated by diffusion, not shear</li> <li>colloid source was modeled as unlimited in these experiments based on successive rainfall simulations</li> </ul>
Schelde et al. (2002)	<ul style="list-style-type: none"> <li>intact cores in laboratory columns</li> <li>sandy loam (moraine deposit), Typic Hapludalf</li> <li>macroporous</li> </ul>	<ul style="list-style-type: none"> <li>simulated Hanford tank water</li> <li>1.0 M NaCl, pH 10 (carbonate-buffered)</li> <li>pH 10 (carbonate-buffered)</li> </ul>	<ul style="list-style-type: none"> <li>rain simulator</li> <li>q = 11 and 30 mm h<sup>-1</sup></li> <li>intervals between rainfall: 0.5 h, 1 d, 7 d</li> </ul>	<ul style="list-style-type: none"> <li>natural colloids</li> </ul>	<ul style="list-style-type: none"> <li>5–4100</li> </ul>	<ul style="list-style-type: none"> <li>colloid mobilization dominated by diffusion, not shear</li> <li>colloid source was modeled as unlimited in these experiments based on successive rainfall simulations</li> </ul>
Cherrey et al. (2003)	<ul style="list-style-type: none"> <li>laboratory column sieved (&lt;2 mm) fraction of Hanford Formation</li> <li>coarse, unconsolidated</li> <li>air-dried</li> </ul>	<ul style="list-style-type: none"> <li>simulated Hanford tank water</li> <li>1.0 M NaCl, pH 10 (carbonate-buffered)</li> <li>pH 10 (carbonate-buffered)</li> </ul>	<ul style="list-style-type: none"> <li>rain simulator</li> <li>Q = 2–90 mL min<sup>-1</sup></li> <li>q = 0.005–4.1 cm min<sup>-1</sup></li> <li>θ = 0.16–1.0</li> </ul>	<ul style="list-style-type: none"> <li>native colloids from Hanford Formation sediments: chlorite, smectite, other clay minerals</li> <li>modified colloids from reacting tank water with sediments: cancrinite, sodalite, other clay minerals</li> <li>EM = -4.0 and -4.5 μm s<sup>-1/2</sup></li> <li>size 350–370 nm mean</li> </ul>	<ul style="list-style-type: none"> <li>C = 10</li> </ul>	<ul style="list-style-type: none"> <li>more rapid colloid breakthrough occurred at lower moisture content</li> <li>greater dispersion of colloid transport occurred at lower moisture content</li> <li>no velocity enhancement (which may be attributed to pore size exclusion) was observed</li> </ul>

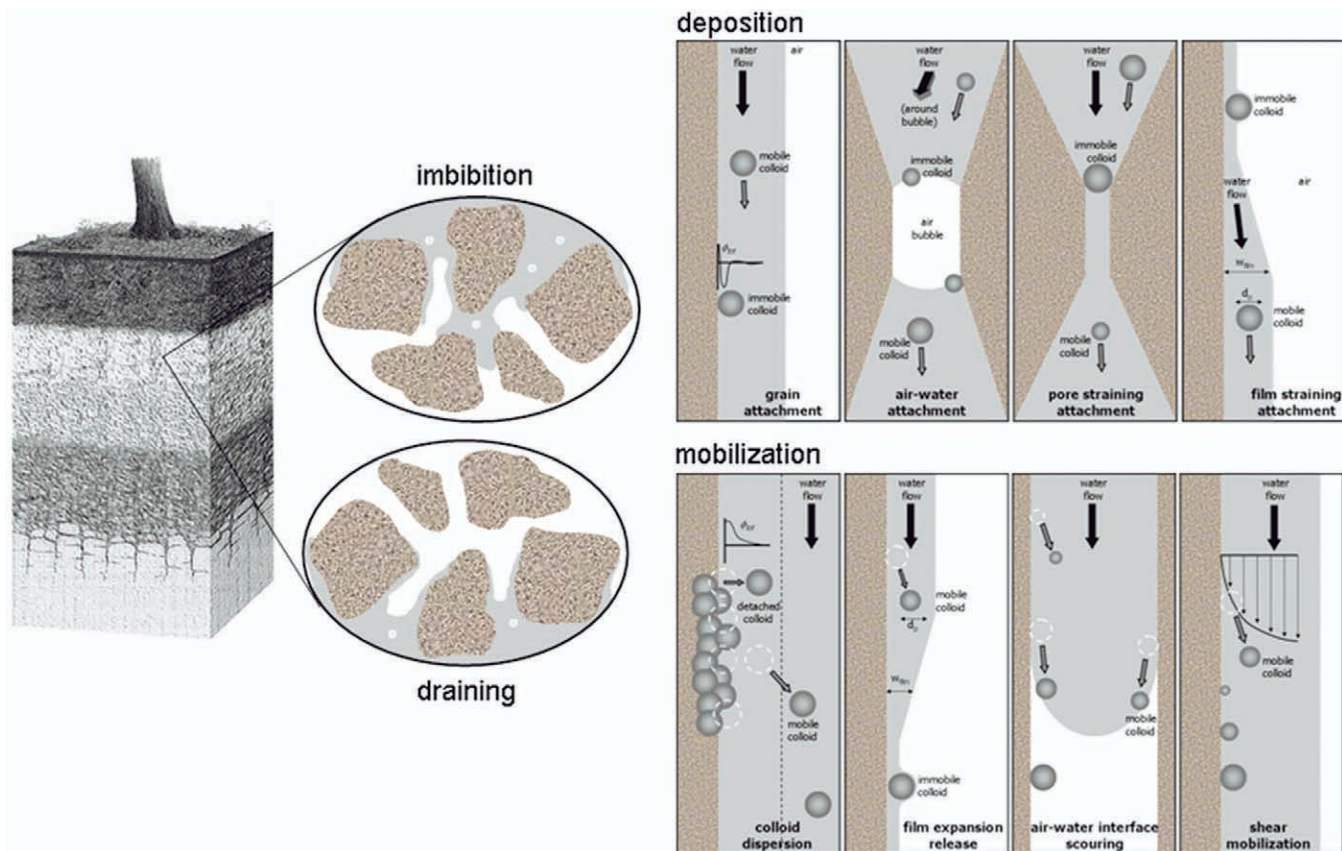


**Fig. 1. Processes affecting colloid movement in unsaturated porous media. Colloid deposition mechanisms include attachment to grains by physicochemical filtration, attachment to immobile air–water interfaces (water flow is around bubble trapped in a pore), attachment by straining in water-saturated pores, and entrapment in thinning water films during draining. Colloid mobilization mechanisms include colloid dispersion by chemical perturbation, expansion of water films during imbibition, air–water interface scouring during imbibition and drainage, and shear mobilization (soil profile from Tarbuck and Lutgens, 1997).**

development of mathematical models that describe colloid transport in these ideal soils. We then explore the application of our understanding of colloid deposition and mobilization in ideal soils to “nonideal” soils, or natural and intact soils that are physically and geochemically heterogeneous (Table 1). We conclude with recommendations for future research.

## COLLOID MOVEMENT IN IDEAL POROUS MEDIA

### Colloid Transport and Deposition

Most experimental studies in ideal porous media have been conducted under conditions of uniform moisture content and steady porewater velocity and have focused on elucidating factors that influence colloid deposition. The experimental results reveal that colloid deposition rates are sensitive to several physical and chemical properties, including volumetric moisture content, flow rate, porewater ionic strength, and colloid size and composition (Wan and Wilson, 1994b; Wan and Tokunaga, 1997; Jewett et al., 1999; Gamedainger and Kaplan, 2001; Saiers and Lenhart, 2003a). The variations in colloid deposition rates with changes in these properties have been attributed to interactions among three deposition mechanisms: mineral-grain attachment, air–water interface capture, and film straining (Fig. 1).

The kinetics of colloid deposition on mineral grains depends on the rate of colloid transport from the bulk fluid to the

grain surface and on the probability that a colloid collision with the mineral grain will succeed in attachment. Colloids are transported from the bulk fluid to the mineral grains by Brownian diffusion, interception, and sedimentation (Yao et al., 1971). The transport rates due to these three mechanisms can be calculated for water-saturated media as functions of the physical properties of the porous medium–water–colloid system, including colloid diameter and density, grain size, and flow velocity (Yao et al., 1971; Rajagopalan and Tien, 1976; Logan et al., 1995; Tufenkji and Elimelech, 2004). An analogous theory for water-unsaturated media is unavailable. Its development relies on improvements in models for air–water configuration in variably saturated porous media and, for natural systems, on consideration of the effects of irregularities in the shapes of the mineral grains and colloids.

Attachment of colloids that strike the mineral grains is determined from the net-interaction potential, which can be calculated from DLVO theory as the sum of the electrostatic double-layer force, the van der Waals force, and short-range solvation or steric forces (Derjaguin and Landau, 1941; Verwey and Overbeek, 1948; McDowell-Boyer et al., 1986; Ryan and Elimelech, 1996). The magnitude and direction of these forces depend on the chemical and physical characteristics of the colloid and soil-grain surfaces and, for the electrical double-layer force, the chemical composition of the porewater. At low ionic strength and for similarly charged colloids and soil grains, the net-interaction potential exhibits a repulsive maximum that hinders the attachment of colloids that approach the mineral-grain surface. With increasing ionic strength,



Table 2. Examples of studies on colloid transport, deposition, and mobilization in ideal porous media under unsaturated conditions. The following variables are used in characterization of the experiments and experimental materials: flow velocity ( $v$ ), volumetric discharge ( $Q$ ), specific discharge ( $q$ ), influent colloid concentration ( $C$ ), ionic strength ( $I$ ), moisture content ( $\Theta$ ), and electrophoretic mobility (EM). Studies conducted under steady flow focus on colloid deposition, while those conducted under transient flow focus on colloid mobilization.

Reference	Porous medium	Water chemistry	Water flow	Colloids	Major results
Wan and Wilson (1994a)	<ul style="list-style-type: none"> <li>porous-medium micromodel, etched glass</li> <li>visualization by optical microscope</li> <li>pore bodies 4–400 <math>\mu\text{m}</math>, pore throats 20–100 <math>\mu\text{m}</math></li> </ul>	<ul style="list-style-type: none"> <li><math>\text{NaNO}_3</math> solution</li> <li><math>I = 1 \text{ mM}</math></li> <li>pH 6.6</li> </ul>	<ul style="list-style-type: none"> <li><math>Q = 1.5\text{--}15 \text{ mL h}^{-1}</math></li> <li>water-saturated</li> <li>unsaturated</li> <li>steady flow</li> </ul>	<ul style="list-style-type: none"> <li>polystyrene latex microspheres: carboxylate (950 nm), sulfate (1050 nm), amidine (600 nm)</li> <li>montmorillonite (<math>\approx 500 \text{ nm}</math>)</li> <li>bacteria: hydrophobic and hydrophilic (about 1000 nm)</li> <li><math>C = 5 \times 10^5 \text{ colloids L}^{-1}</math></li> </ul>	<ul style="list-style-type: none"> <li>colloids sorbed to air–water interface and solid–water interfaces</li> <li>hydrophobic colloids (by contact angle) sorbed to a greater extent than hydrophilic colloids to air–water interfaces</li> <li>sorption at air–water interface was irreversible</li> </ul>
Wan and Wilson (1994b)	<ul style="list-style-type: none"> <li>laboratory column</li> <li>quartz sand (0.21–0.32 mm)</li> </ul>	<ul style="list-style-type: none"> <li><math>\text{NaNO}_3</math> solution</li> <li><math>I = 1 \text{ mM}</math></li> <li>pH 6.6</li> </ul>	<ul style="list-style-type: none"> <li><math>v = 10 \text{ cm h}^{-1}</math></li> <li><math>\Theta = 0.23\text{--}0.43</math></li> <li>steady flow</li> </ul>	<ul style="list-style-type: none"> <li>polystyrene latex microspheres: “hydrophobic” sulfate (220 nm), “hydrophilic” carboxylate (190 nm)</li> <li><math>C = 5 \times 10^5 \text{ colloids L}^{-1}</math></li> </ul>	<ul style="list-style-type: none"> <li>retention of hydrophilic and hydrophobic colloids increased with porous-medium air content</li> <li>retention increased with degree of colloid surface hydrophobicity</li> <li>moving air–water interfaces may have affected colloid transport</li> </ul>
Wan and Tokunaga (1997)	<ul style="list-style-type: none"> <li>laboratory column</li> <li>quartz sand:</li> <li>0.15–0.21 mm,</li> <li>0.21–0.43 mm,</li> <li>0.43–0.50 mm</li> </ul>	<ul style="list-style-type: none"> <li><math>\text{NaCl}</math> solution</li> <li><math>I = 1.0 \text{ mM}</math></li> <li>pH 5.5</li> </ul>	<ul style="list-style-type: none"> <li><math>q = 0.004 \text{ to } 340 \text{ cm h}^{-1}</math></li> <li><math>\Theta = 0.08\text{--}0.35</math></li> <li>steady flow</li> </ul>	<ul style="list-style-type: none"> <li>polystyrene latex microspheres: 14, 93, 280, 970 nm in diameter</li> <li><math>C = 1.1\text{--}10.1 \times 10^5 \text{ colloids L}^{-1}</math></li> </ul>	<ul style="list-style-type: none"> <li>increased colloid breakthrough with increased moisture content</li> <li>colloid removal dominated by film straining at low moisture content</li> <li>increased film straining efficiency with decreased grain size</li> <li>increased film straining efficiency with increased colloid size</li> </ul>
Schäfer et al. (1998)	<ul style="list-style-type: none"> <li>laboratory column</li> <li>quartz sand (0.25–0.5 mm)</li> </ul>	<ul style="list-style-type: none"> <li>phosphate-buffered saline solution</li> <li><math>I = 10 \text{ mM}</math></li> <li>pH 7.2</li> </ul>	<ul style="list-style-type: none"> <li><math>v = 1.5\text{--}2 \text{ cm min}^{-1}</math></li> <li><math>\Theta = 0.22\text{--}0.41</math></li> <li>steady flow</li> </ul>	<ul style="list-style-type: none"> <li>two bacterial strains: <i>Rhodococcus</i> sp. C125 and P. <i>putida</i> mt2</li> </ul>	<ul style="list-style-type: none"> <li>bacterial affinity for air–water interfaces was greater than for solid–water interfaces</li> <li>bacterial retention within column varied inversely with moisture content</li> </ul>
Chu et al. (2001)	<ul style="list-style-type: none"> <li>packed columns</li> <li>clean quartz sand</li> <li>iron oxide-coated sand</li> </ul>	<ul style="list-style-type: none"> <li>phosphate-buffered saline solution</li> <li>pH 7.5</li> </ul>	<ul style="list-style-type: none"> <li><math>q = 1.1\text{--}4.9 \text{ cm h}^{-1}</math></li> <li><math>\Theta = 0.09\text{--}0.33</math></li> <li>steady flow</li> </ul>	<ul style="list-style-type: none"> <li>MS2 and <math>\Phi\text{X174}</math> bacteriophages</li> </ul>	<ul style="list-style-type: none"> <li>bacteriophages displayed little affinity for air–water interfaces in the presence of reactive solid surfaces</li> <li>reductions in moisture content increased bacteriophage deposition onto solid–water interfaces</li> </ul>
Gamerding and Kaplan (2001)	<ul style="list-style-type: none"> <li>laboratory centrifuge column</li> <li>quartz sand (0.59–0.85 mm)</li> </ul>	<ul style="list-style-type: none"> <li>deionized water</li> <li>carbonate/bicarbonate solution</li> <li><math>I = 12 \text{ mM}</math></li> <li>pH 7.8</li> </ul>	<ul style="list-style-type: none"> <li>flow driven by centrifugation</li> <li><math>\Theta = 0.06\text{--}0.19</math></li> <li>steady flow</li> </ul>	<ul style="list-style-type: none"> <li>polystyrene latex microspheres (280 nm, carboxyl-modified)</li> <li><math>C = 4.5 \text{ mg L}^{-1}</math></li> </ul>	<ul style="list-style-type: none"> <li>increased colloid breakthrough with decreased ionic strength</li> <li>increased colloid breakthrough with increased moisture content</li> </ul>
Lenhart and Saiters (2002)	<ul style="list-style-type: none"> <li>laboratory column</li> <li>quartz sand (0.30–0.35 mm)</li> </ul>	<ul style="list-style-type: none"> <li><math>\text{NaHCO}_3/\text{NaCl}</math> water solution</li> <li><math>I = 1 \text{ mM}</math></li> <li>pH 7.4</li> </ul>	<ul style="list-style-type: none"> <li><math>v = 9\text{--}117 \text{ cm h}^{-1}</math></li> <li><math>\Theta = 0.09\text{--}0.34</math></li> <li>steady flow</li> </ul>	<ul style="list-style-type: none"> <li>silica (360 nm)</li> <li><math>C = 100 \text{ mg L}^{-1}</math></li> </ul>	<ul style="list-style-type: none"> <li>colloid breakthrough increased with increasing moisture content</li> <li>colloid breakthrough depended on wetting history</li> <li>dominant mechanism of colloid retention changed from straining to air–water interface capture as moisture content increased</li> </ul>
Saiters and Lenhart (2003b)	<ul style="list-style-type: none"> <li>laboratory column</li> <li>quartz sand (0.30–0.36 mm)</li> </ul>	<ul style="list-style-type: none"> <li><math>\text{NaHCO}_3/\text{NaCl}</math> water</li> <li><math>I = 1 \text{ mM}</math></li> <li>pH 7.4</li> </ul>	<ul style="list-style-type: none"> <li><math>q = 0.01\text{--}0.5 \text{ cm min}^{-1}</math></li> <li>transient flow</li> </ul>	<ul style="list-style-type: none"> <li>silica colloids</li> <li>size 360 nm</li> <li>EM <math>-3.6 \mu\text{m s}^{-1} \text{ cm V}^{-1}</math></li> <li>mobilization of 20–100 <math>\text{mg L}^{-1}</math></li> </ul>	<ul style="list-style-type: none"> <li>colloid mobilization occurred rapidly while wetting front is passing</li> <li>fraction of colloids eligible for mobilization depended on moisture content</li> <li>colloid-mobilization kinetics were sensitive to porewater velocity</li> </ul>
Saiters and Lenhart (2003a)	<ul style="list-style-type: none"> <li>laboratory column</li> <li>quartz sand (0.30–0.36 mm)</li> </ul>	<ul style="list-style-type: none"> <li><math>\text{NaHCO}_3/\text{NaCl}</math> water</li> <li><math>I = 0.2\text{--}200 \text{ mM}</math></li> <li>pH 7.3</li> </ul>	<ul style="list-style-type: none"> <li><math>q = 0.66 \text{ cm min}^{-1}</math></li> <li><math>\Theta = 0.36</math></li> <li>steady flow</li> </ul>	<ul style="list-style-type: none"> <li>silica (360 nm)</li> <li><math>C = 100 \text{ mg L}^{-1}</math></li> </ul>	<ul style="list-style-type: none"> <li>transition of removal mechanisms from film straining to air–water interface capture to mineral–water interface attachment with increasing ionic strength</li> <li>overall removal increased with increasing ionic strength</li> </ul>
Saiters et al. (2003)	<ul style="list-style-type: none"> <li>laboratory column</li> <li>quartz sand (0.71–0.85 mm)</li> </ul>	<ul style="list-style-type: none"> <li><math>\text{NaHCO}_3/\text{NaCl}</math> water</li> <li><math>I = 0.1\text{--}50 \text{ mM}</math></li> <li>pH 7.4</li> </ul>	<ul style="list-style-type: none"> <li><math>Q = 49 \text{ mL h}^{-1}</math> and 16–146 <math>\text{mL h}^{-1}</math></li> <li>transient flow</li> </ul>	<ul style="list-style-type: none"> <li>kaolinite</li> <li>mobilization of 10 to <math>&gt;50 \text{ mg L}^{-1}</math></li> </ul>	<ul style="list-style-type: none"> <li>moving air–water interfaces associated with drying fronts mobilized colloids</li> <li>amount of mobilized colloids increased as the velocity of the downward-propagating air–water interface increased</li> <li>amount of mobilized colloids decreased with increasing ionic strength</li> </ul>

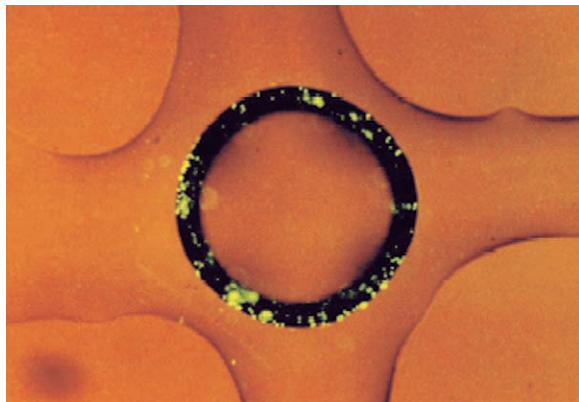


**Fig. 2. Negatively charged latex colloids (0.95  $\mu\text{m}$ ) deposited preferentially onto an air bubble trapped in a pore body of a porous-medium micromodel (from Wan and Wilson, 1994a).**

the repulsive barrier decreases in magnitude, which increases the probability that a colloid-grain collision will succeed in colloid attachment. The repulsive barrier is absent for oppositely charge colloids and soil grains, in which case the deposition rate is controlled by the rate at which colloids are transported from the pore fluid to the mineral-grain surface.

Predictions of colloid deposition that are based on DLVO theory have not been published for water-unsaturated systems, but DLVO theory has been tested against measurements of colloid deposition in water-saturated porous media. These evaluations show that theoretically determined deposition rates substantially underestimate corresponding measured values when repulsive barriers exist between the colloids and mineral grains (Elimelech et al., 1995). Agreement between DLVO-based and laboratory-measured deposition rates has been improved through recent modifications to theory that account for complexities associated with surface-charge heterogeneity, grain-scaled surface roughness, and deposition within the secondary minimum of the net-interaction energy profile (Bhattacharjee et al., 1998; Hahn and O'Melia, 2004). These modifications, although designed to improve descriptions of colloid deposition in water-saturated media, should also be applicable for quantifying colloid deposition reactions on mineral-grain surfaces present within unsaturated porous media.

Like the soil surfaces, air–water interfaces present within unsaturated porous media can serve as collectors of colloidal particles (Fig. 1 and 2). Colloids that are transported to the air–water interface are retained by either capillary or electrostatic forces; therefore, colloid capture at air–water interfaces depends on pH, ionic strength, and colloid surface properties. Increases in ionic strength reduce the magnitude of the repulsive energy barrier between the negatively charged air–water interface and like-charged mineral colloids, leading to progressively more favorable conditions for attachment and faster rates of air–water interface capture (Wan and Wilson, 1994a; Saiers and Lenhart, 2003a). Hydrophobic colloids, such as certain bacteria, exhibit a greater affinity for air–water interfaces than mineral colloids, which have comparatively hydrophilic surfaces (Wan and Wilson, 1994b; Schäfer et al., 1998; Lenhart and Saiers, 2002). Among clay-mineral colloids, the affinity for the air–water interfaces depends on the colloid shape and surface-charge distribution and varies inversely with colloid cation-exchange capacity. Kaolinite partitions more strongly to the air–water interface than illite, while bentonite and montmorillonite exhibit negligible partitioning (Wan and Tokunaga, 2002).

Straining occurs within mobile-water conduits that are too narrow to permit colloids to pass (Fig. 1). Early studies on the removal of colloids by pore straining in water-saturated porous media showed that colloids were retained if their diam-

eter exceeded about one-twentieth to one-tenth the diameter of the porous media grains (Sakthivadivel, 1966; Herzog et al., 1970). More recent studies motivated by the need to better understand the removal of protozoan cysts during riverbank filtration have explored the pore straining of polystyrene microspheres in uniform and poorly sorted porous media (Bradford et al., 2002, 2003). This recent work showed that pore straining can be modeled as first-order removal with a rate coefficient that depends on the depth and mean grain diameter of the porous media. Pore straining may also contribute to colloid immobilization within small, water-filled pore spaces present within unsaturated porous media. In partially saturated pores with dimensions that exceed those of the colloids, film straining may remove colloids from the mobile phase. According to Wan and Tokunaga (1997), colloid immobilization by film straining depends on the probability of pendular ring discontinuity and on the ratio of colloid size to film thickness (a pendular ring is water held by surface tension near the contacts of adjacent mineral grains). The probability of pendular ring discontinuity increases from zero to unity as the capillary pressure decreases (i.e., as the porous medium drains). As pendular rings disconnect, an increasing proportion of water flow and colloid transport is relegated to the adsorbed films of water that envelop the mineral grains. When film width is greater than colloid diameter, straining does not occur. When film width is similar to or less than the colloid diameter, however, surface tension retains colloids against the mineral grain surfaces.

The relative importance of soil-grain attachment, air–water interface capture, and film straining to colloid deposition is not constant, but varies as a function of porewater chemistry, moisture content, and colloid characteristics. The work of Wan and Tokunaga (1997) and Lenhart and Saiers (2002) suggests that film straining represents the most important deposition mechanism for hydrophilic colloids under conditions of low ionic strength ( $<10^{-3} M$ ) and low to intermediate moisture content. As moisture content and ionic strength increase, the leading colloid deposition mechanism may transition from film straining to air–water interface capture or soil grain attachment, depending on the surface characteristics of the colloids and mineral grains (Saiers and Lenhart, 2003a).

### Modeling Colloid Transport and Deposition

The observations reviewed above have been instrumental in guiding the development of mathematical models for colloid transport and deposition within homogeneous granular materials. Most of these transport and deposition models are based on the assumption of steady porewater flow and conceptualize the unsaturated porous medium as a three-component system consisting of air, water, and mineral grains (e.g., Sim and Chrysikopoulos, 2000). Colloids are transmitted through the water-filled sections of the porous medium by advection and dispersion and are removed from the porewater by straining, air–water interface capture, and deposition onto soil–water interfaces. Film straining and air–water interface capture are treated as irreversible mass-transfer processes, a suitable approximation provided that flow and porewater chemistry remain steady (Corapcioglu and Choi, 1996; Wan and Tokunaga, 1997). Colloid release from soil–water interfaces is often accommodated in unsaturated transport models, but is generally slow in the absence of hydrologic and chemical perturbations (Schäfer et al., 1998; Chu et al., 2001).

The advection–dispersion equation describes the movement of porewater colloids. The one-dimensional form of this equation is given by

$$\frac{\partial C}{\partial t} + \frac{\partial \Gamma_{STR}}{\partial t} + \frac{\rho_c}{S_w} \left[ f_{air} \frac{\partial \Gamma_{AWI}}{\partial t} + f_{soil} \frac{\partial \Gamma_{SWI}}{\partial t} \right] = A_L \nu \frac{\partial^2 C}{\partial z^2} - \nu \frac{\partial C}{\partial z} \quad [1]$$

where  $C$  is the porewater colloid concentration;  $\Gamma_{STR}$ ,  $\Gamma_{AWI}$ , and  $\Gamma_{SWI}$  are immobile-phase colloid concentrations for removal by film straining (STR) air–water interface capture (AWI), and soil–water interface deposition (SWI);  $t$  is time;  $\rho_c$  is the ratio of colloid mass to its effective cross-sectional area;  $S_w$  is water saturation;  $f_{air}$  is the air–water interfacial area per unit void volume;  $f_{soil}$  is the soil–water interfacial area per unit void volume;  $A_L$  is the longitudinal dispersivity;  $\nu$  is the average porewater velocity; and  $z$  is the coordinate parallel to flow. The concentration of strained colloids ( $\Gamma_{STR}$ ) is expressed in terms of colloid mass per volume of porewater, while  $\Gamma_{AWI}$  and  $\Gamma_{SWI}$  are expressed in terms of normalized surface coverages (i.e., area of attached colloids per area of interface). Solution of Eq. [1] requires specification of the kinetics expressions for film straining, air–water interface capture, and deposition onto soil–water interfaces.

Wan and Tokunaga (1997) quantified colloid straining inside thin films with a first-order kinetics expression:

$$\frac{\partial \Gamma_{STR}}{\partial t} = k_{STR} C \quad [2]$$

where  $k_{STR}$ , the rate coefficient for film straining, varies according to

$$k_{STR} = P(\Psi) \left( \frac{d}{w} \right)^\beta N \nu^{(1+h)} \quad [3]$$

In Eq. [3],  $P(\Psi)$  is the probability of pendular ring discontinuity (expressed as a function of matric potential,  $\Psi$ ),  $d$  is the colloid diameter, set  $w$  is the film thickness,  $h$ ,  $N$ , and  $\beta$  are empirical parameters. Wan and Tokunaga (1997) employed Eq. [2] and [3] to describe film straining rates in a suite of column experiments that were conducted at matric potentials ranging from  $-0.05$  to  $-0.5$  m and with microspheres ranging in diameter from  $0.014$  to  $0.97$   $\mu\text{m}$ .

Colloids traveling within relatively large water channels (e.g., interconnected pendular rings) are not affected by film straining, but they may diffuse to the air–water interface where electrostatic or capillary forces retain them. A second-order kinetics expression has been invoked to describe the attachment of microspheres, bacteria, viruses, and mineral colloids at air–water interfaces present within porous media (Corapcioglu and Choi, 1996; Schäfer et al., 1998; Chu et al., 2001). The formulation of this rate law varies slightly depending on whether the captured colloid mass is normalized by the volume of air or by air–water interfacial area. For the case of normalization by interfacial area, the rate law is expressed by

$$\frac{\rho_c}{S_w} f_{air} \frac{\partial \Gamma_{AWI}}{\partial t} = k_{AWI} \eta_{AWI} C \quad [4a]$$

where  $k_{AWI}$  is a rate coefficient for air–water interface capture and  $\eta_{AWI}$  is a blocking function. The blocking function declines linearly as  $\Gamma_{AWI}$  increases:

$$\eta_{AWI} = 1 - \lambda_{AWI} \Gamma_{AWI} \quad [4b]$$

where  $\lambda_{AWI}$  is an excluded area parameter equivalent to the ratio of blocked air–water interfacial area to the projected cross-sectional area of the colloid. Inspection of Eq. [4a] and [4b] shows that colloid capture rates vary linearly with  $C$  and decline as colloids accumulate on the air–water interface.

The magnitude of  $k_{AWI}$  depends on the rate of colloid transport from the bulk fluid phase to the air–water interface and on the probability that a colloid collision with the interface will result in attachment. While neither the transport rate nor

the attachment probability can be accurately determined on a theoretical basis, discernible trends between the magnitude of  $k_{AWI}$  and some system properties have been identified. In particular, values of  $k_{AWI}$  that quantify silica-colloid attachment vary proportionately with the one-third power of the porewater velocity ( $k_{AWI} \propto \nu^{1/3}$ ) (Lenhart and Saiers, 2002) and increase linearly with porewater ionic strength (Saiers and Lenhart, 2003a).

The reciprocal of  $\lambda_{AWI}$  ( $\lambda_{AWI}^{-1}$ ) defines the maximum attainable surface coverage at the air–water interface. Estimates of  $\lambda_{AWI}^{-1}$  increase with ionic strength because of a reduction in repulsive electrical double layer forces between colloids. Even at elevated ionic strengths, maximum surface coverages for both biocolloids and mineral colloids are low. For example, Abdel-Fattah and El-Genk (1998) reported  $\lambda_{AWI}^{-1}$  values for hydrophobic microsphere ranging from 0.012 to 0.08 for ionic strengths between 0.001 and 1  $M$ , while Saiers and Lenhart (2003a) reported  $\lambda_{AWI}^{-1}$  values for silica colloids ranging from 0.001 to 0.03 for ionic strengths between  $2 \times 10^{-4}$  and 0.2  $M$ . The parameter  $\lambda_{AWI}^{-1}$  likely depends on hydrodynamic forces in addition to forces between colloids (Ko and Elimelech, 2000). Because hydrodynamic forces vary with position along the air–water interface, colloid surface coverages are undoubtedly nonuniform, with some areas of the air–water interface completely devoid of colloids (even at maximum surface coverages), while other areas collect colloids in high concentrations. Estimates of  $\lambda_{AWI}^{-1}$ , then, should be regarded as a spatial average over the entire air–water interface.

Methods for quantifying soil–water interface reactions in unsaturated media are largely based on approaches derived from studies conducted in water-saturated systems. Several investigators have adopted a second-order reversible rate law to describe colloid mass-transfer reactions with the solid phase (Corapcioglu and Choi, 1996; Schäfer et al., 1998; Chu et al., 2001):

$$\frac{\rho_c}{S_w} f_{soil} \frac{\partial \Gamma_{SWI}}{\partial t} = k_{SWI} \eta_{SWI} C - \frac{\rho_c}{S_w} f_{soil} k_R \Gamma_{SWI} \quad [5a]$$

$$\eta_{SWI} = 1 - \lambda_{SWI} \Gamma_{SWI} \quad [5b]$$

where  $k_{SWI}$  is a rate coefficient for colloid deposition onto the mineral grains,  $k_R$  is a rate coefficient for colloid release, and  $\lambda_{SWI}$  is an excluded area parameter. Application of this kinetics formulation to data on microsphere, virus, and bacteria transport indicate that  $k_R$  is small or zero, at least for conditions of constant flow and porewater chemistry. Like their air–water interface counterparts,  $k_{SWI}$  and  $\lambda_{SWI}$  are sensitive to porewater chemistry, soil composition, and colloid type (Corapcioglu and Choi, 1996; Schäfer et al., 1998; Chu et al., 2001). The deposition rate coefficient ( $k_{SWI}$ ) should exhibit an additional dependence on volumetric moisture content because changes in air–water configuration that accompany variation in moisture content will affect colloid trajectories around (and the transport rate to) the mineral-grain surfaces.

Equations [1], [2], and [4a] to [5b] with unknowns  $C$ ,  $\Gamma_{STR}$ ,  $\Gamma_{AWI}$ , and  $\Gamma_{SWI}$  are suitable for simulating colloid transport, film straining, air–water interface capture, and mineral-grain attachment in unsaturated, homogeneous porous media. Published models that incorporate one or more of these three mass-transfer mechanisms have successfully reproduced data from laboratory experiments on the transport of both inorganic and organic colloids in ideal porous media. Though very encouraging, these results should not be taken as evidence that the colloid-transport problem has been solved. The published simulations rely on adjustment of model parameters that cannot be determined on a theoretical basis and hence the favor-



able model-data agreement should not be considered definitive proof of positive identification of the mechanisms that govern colloid mass transfer. Alternative interpretations of the experimental observations are possible.

### Colloid Mobilization

Few experimental or theoretical studies on colloid mobilization within ideal unsaturated media are available. On the basis of studies with saturated porous media, we anticipate that perturbations in porewater chemistry will promote colloid release (Fig. 1). Ionic-strength reductions and pH increases are the most common chemical perturbations that mobilize colloids in saturated systems (McDowell-Boyer, 1992; Ryan and Gschwend, 1994; Grolimund and Borkovec, 1999) and are likely to play an important role in colloid mobilization within unsaturated systems.

Physical perturbations in flow that characterize typical infiltration events also drive colloid mobilization. Several mechanisms for this flow-induced mobilization have been proposed (Fig. 1). Colloids trapped in narrow porewater conduits (by straining) may be released into the pore fluid when these flow paths expand during soil imbibition (Fig. 3; Saiers and Lenhart, 2003b). Moving air–water interfaces associated with wetting and drying fronts may scavenge colloids from mineral-grain surfaces and facilitate their transport through the porous medium (Gomez-Suarez et al., 1999, 2001; Saiers et al., 2003). Increases in shear stress that accompany porewater-velocity increases may cause colloids to roll along the surface to which they are attached, and these colloids may be released into the porewater upon encountering surface roughness that reduces the DLVO adhesion force (Hubbe, 1985).

### COLLOID MOVEMENT IN NONIDEAL POROUS MEDIA

Findings from ideal systems have been used to identify key mechanisms that influence colloid-deposition kinetics in natural vadose-zone environments and to define, at least qualitatively, how colloid mobility in soils and sediments responds to changes in measurable properties, such as moisture content, porewater chemistry, and flow velocity. However, natural geologic environments are more heterogeneous than ideal systems. Although the soils of some vadose-zone systems exhibit a narrow distribution in pore sizes and are characterized by weak structure, abiotic and biotic processes lead to the creation of macropores (e.g., root channels, worm borrows, desiccation cracks) and aggregation of primary mineral particles in many near-surface soils. This soil structure complicates descriptions of colloid transport because it produces nonuniformity in the velocity of infiltrating water (Beven and Germann, 1982; Selker et al., 1999). Therefore, mathematical models developed for ideal porous media that are based on the assumption of uniform flow cannot be used without modification to quantify colloid movement through macroporous or aggregated soils. In addition to heterogeneity in porous-medium physical properties, the geologic solids of real vadose-zone environments exhibit substantial geochemical heterogeneity. Consequently, the distribution in the rates of colloid mass-transfer reactions may be broader than those measured in experiments with ideal porous media.

### Experimental Findings

Colloid movement through nonideal porous media has been measured in small-scale field experiments and in laboratory experiments with intact soil cores. These experiments most often involve applying water to the surface of the soil and

measuring the concentrations of colloids in water samples collected in lysimeters installed within the soil profile (for field experiments) or at the base of the core (for laboratory experiments). Results of these studies have been instrumental in improving our understanding of factors that control the mobilization of naturally occurring soil colloids.

A salient characteristic of these field and intact soil laboratory experiments is the consistent occurrence of a pulse of colloids at the beginning, and sometimes at the end, of a rainfall event with an interlude of relatively steady colloid mobilization (e.g., Kaplan et al., 1993; Jacobsen et al., 1997; Ryan et al., 1998; El-Farhan et al., 2000). The colloid pulses during imbibition and draining can be attributed to the effect of flow transients on colloid mobilization. The relatively steady colloid mobilization during the rainfall event can be attributed to the gradual propagation of chemical (and perhaps some physical) perturbations through the soil column.

The best example of colloid mobilization pulses coinciding with the beginning and end of a simulated rainfall event is provided by the field experiments conducted by El-Farhan et al. (2000). Infiltrating water was applied as water ponded on the soil surface. Peak colloid concentrations (up to 265 mg L<sup>-1</sup>) were recorded in the first few and last few samples of water taken from zero-tension lysimeters at 25-cm depths (Fig. 4). These peak concentrations were attributed to the passage of colloid-scavenging air–water interfaces during imbibition and draining. The experiments conducted by Saiers et al. (2003) in ideal porous media reinforce this interpretation for the draining. In addition, some of the pulse of colloid mobilization that occurs at the beginning of a rainfall event can be attributed to the release of colloids into expanding of water films (Saiers and Lenhart, 2003b).

Following the pulse of colloid mobilization typically observed during imbibition, colloid concentrations are often relatively steady (El-Farhan et al., 2000) or they gradually decrease with time (Kaplan et al., 1993; Jacobsen et al., 1997; Ryan et al., 1998; Schelde et al., 2002). The colloid mobilization behavior observed during steady rainfall infiltration has frequently been interpreted as control of colloid mobilization kinetics by colloid diffusion. Colloid mobilization can be viewed as a two-step process involving (i) detachment of colloids from soil grain and aggregate surfaces and (ii) diffusion of colloids from the detachment site to the mobile porewater. The diffusion step may be envisioned as diffusive transport through a layer of immobile water in which diffusive transport of colloids is more important than advective transport (Ryan and Gschwend, 1994). The diffusion step can also be viewed as diffusion through two regions, one being a soil “crust” representing soil aggregates or soil matrix, and the other being the immobile water layer (Schelde et al., 2002).

In nonideal porous media, there are indications that the detachment step is promoted by various chemical and physical perturbations (e.g., decreasing ionic strength, increasing pH, shear stress), with the addition of another chemical perturbation, the detachment of colloids by dissolution of mineral cements that bind together various soil constituents (e.g., Harris et al., 1987; Weisbrod et al., 2002). Despite these indications, experiments in nonideal porous media have not yielded much insight into detachment mechanisms because it is highly unlikely that the detachment kinetics would be the rate-limiting step in an experiment in which a measurable amount of colloids were mobilized. Instead, most of these experiments show that kinetics of colloid mobilization during steady infiltration appears to be limited by the diffusion step (Jacobsen et al., 1997; Lægdsmand et al., 1999; Schelde et al., 2002).

The key experimental result that supports an interpretation of diffusion-limited kinetics for colloid mobilization is a linear



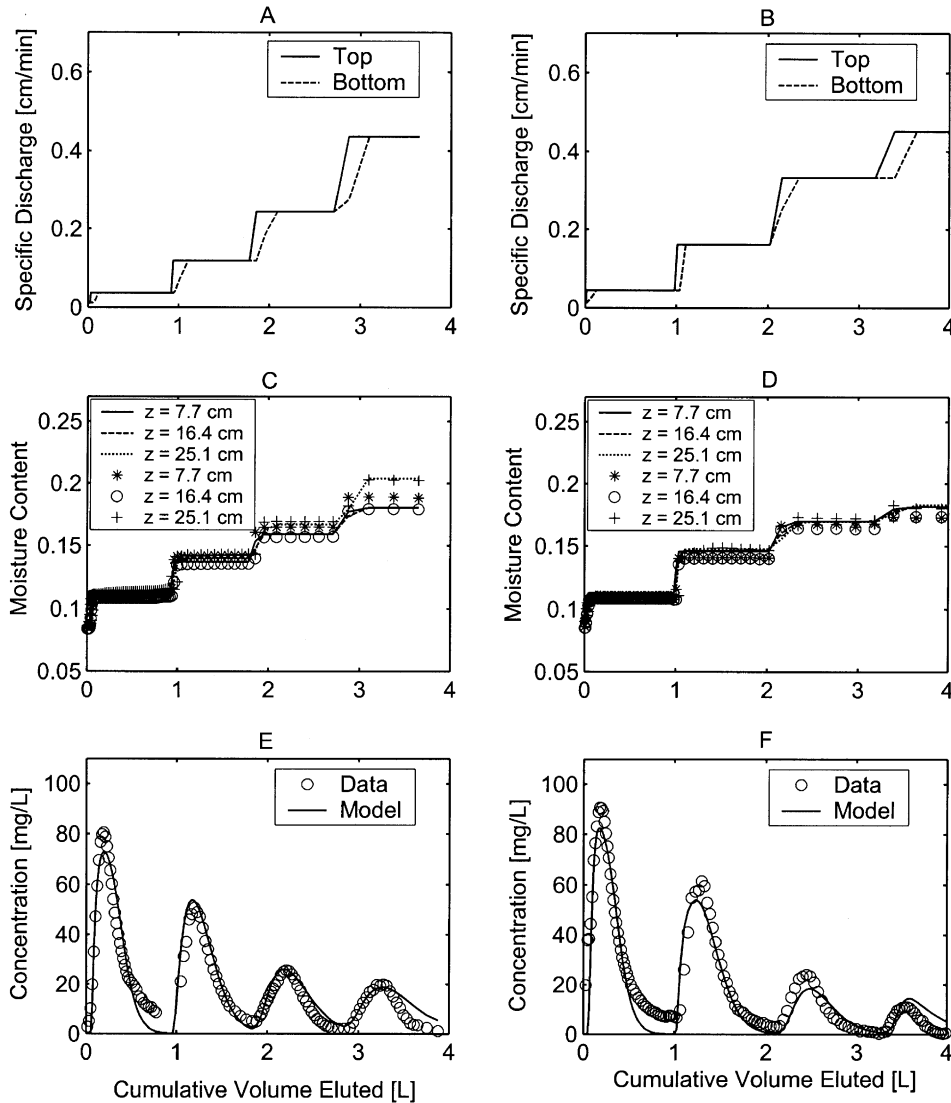


Fig. 3. Model-computed results and those measured in duplicate experiments on silica-colloid mobilization from columns of quartz sand: (A,B) measured specific discharge at column boundaries, (C,D) measured moisture content (symbols) and modeled moisture content (lines) for three positions along the 32-cm-long columns ( $z = 0$  at column top), and (E,F) colloid breakthrough pulses generated by successive increases in flow rate (from Sainers and Lenhart, 2003b).

relationship between the cumulative mass of mobilized colloids and the square root of time (Fig. 5) following

$$M_t = 4M_\infty l \sqrt{\frac{D_c t}{\pi}} \quad [6]$$

where  $M_t$  is the cumulative mass of mobilized colloids as a function of time  $t$ ,  $M_\infty$  is the total mass of colloids that can be mobilized in a sheet of thickness  $l$ , and  $D_c$  is the diffusion coefficient of the colloid (Crank, 1975). Such linear relationships were observed by Jacobsen et al. (1997), Lægdsmand et al. (1999), and Schelde et al. (2002) for intact soils in laboratory columns.

Under some conditions, the linear relationship between cumulative mass and the square root of time has not been observed. For example, both Jacobsen et al. (1997) and Lægdsmand et al. (1999) noted deviations from the linear relationship for early time (during imbibition) and for high flow rates. These deviations indicate that processes other than diffusion may control colloid mobilization kinetics under these conditions. During imbibition, colloid scavenging by air-water interfaces

may be dominating colloid mobilization. At high flow rates, shear stress may affect colloid mobilization kinetics. In model systems of spherical colloids attached to flat plates, the force of hydrodynamic shear ( $F_H$ ) is proportional to the flow velocity  $V_R$  at the height of the colloid radius  $R$  and the radius of the colloids (O'Neill, 1968):

$$F_H = (1.7)6\pi\mu RV_R \quad [7]$$

where  $\mu$  is the dynamic viscosity of the fluid. The shear force is opposed by an adhesive force, which is described by DLVO interactions. Kaplan et al. (1993) and Lægdsmand et al. (1999) found support for mobilization by shear in positive correlations between mobilized colloid concentrations and flow rate by assuming that the velocity of infiltrating water is proportional to flow rate and the concentration of colloids is proportional to the shear force. Similarly, Weisbrod et al. (2002) reported a power law relationship between the flow rate and the amount of colloids mobilized from a fractured chalk formation.

### Modeling Colloid Mobilization in Nonideal Media

Efforts are just beginning to build a modeling framework appropriate for describing the mobilization and transport of colloids in nonideal, unsaturated porous media (Jarvis et al., 1999; Schelde et al., 2002). These colloid-transport models, like those developed for ideal systems, ignore the effects of biological processes (e.g., growth, decay, predation, and inactivation) and thus are most appropriately applied to the movement of inorganic colloids.

Schelde et al. (2002) developed a model capable of simulating the mobilization and transport of natural mineral colloids within macroporous soils cores (Fig. 6). This model is similar in form to dual-porosity, mobile-immobile models for solute transport in structured and aggregated porous media (Coats and Smith, 1964; van Genuchten and Cleary, 1979; Nkedi-Kizza et al., 1984). It accounts for an equivalent macropore

that approximates the average behavior of the actual macropore network. Water in the partially saturated macropore is assumed to occur as a thin film with mobile- and immobile-water portions. Colloids are generated from a "crust layer" near the macropore edge. These colloids presumably diffuse across the stagnant portion of the water film and enter its mobile-water portion, where flow is steady and the colloids are transported by advection and dispersion. Although Schelde et al. (2002) developed this model in the context of macroporous soils, it could be applied to describe colloid transport and mass transfer in aggregated soils by conceptualizing the water in the aggregates as immobile water and the water in the interaggregate pore spaces as the mobile water.

The model of Jarvis et al. (1999) shares the two-domain conceptualization embodied in the model of Schelde et al. (2002), but accounts for transient porewater flow in both the macroporous and microporous regions of the soil. This model

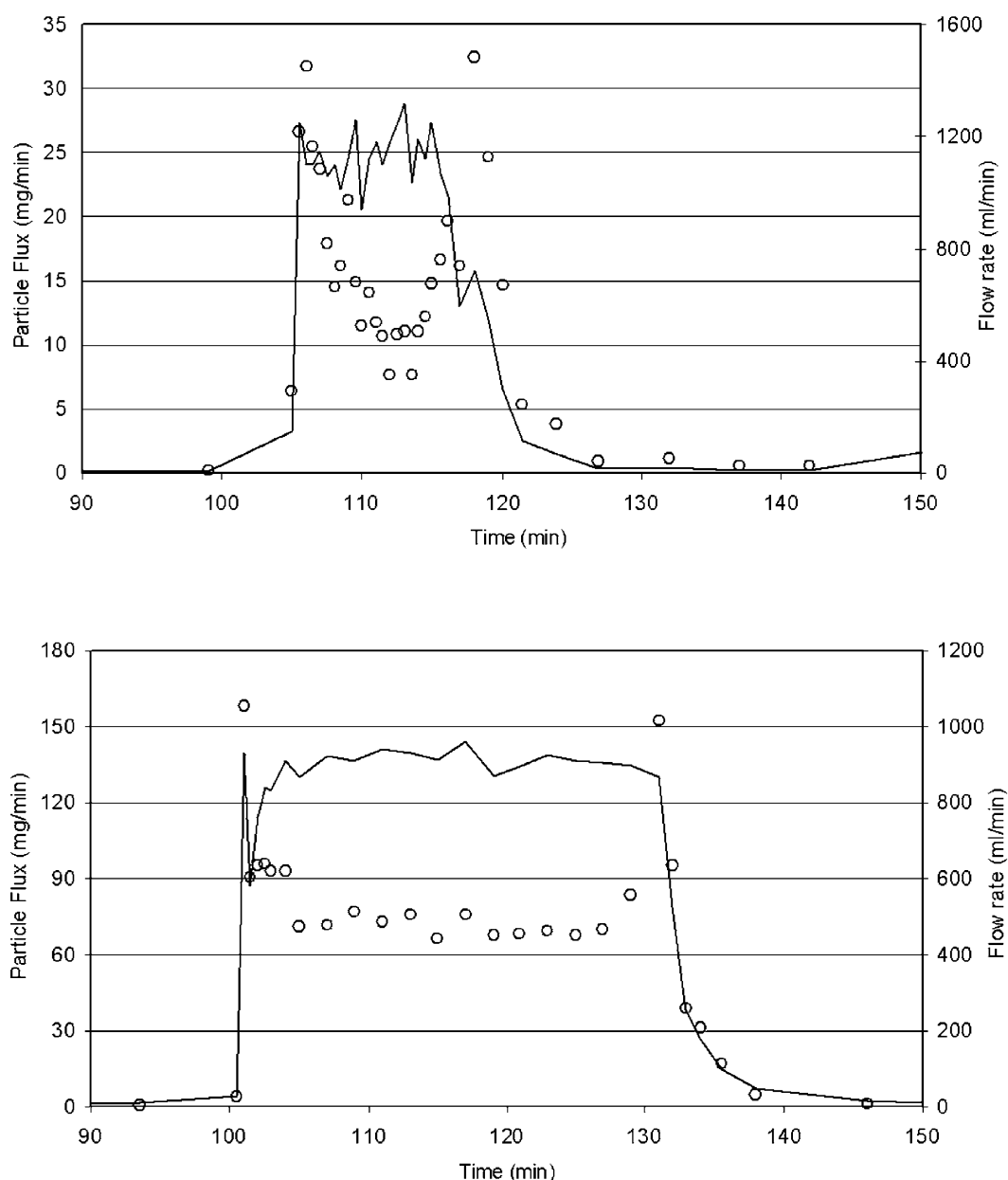


Fig. 4. Colloid mass flux (filled circles) and porewater flow rates (solid lines) measured during two ponded infiltration experiments. Colloid concentrations peak during the passage of both wetting and drying fronts (from El-Farhan et al., 2000).

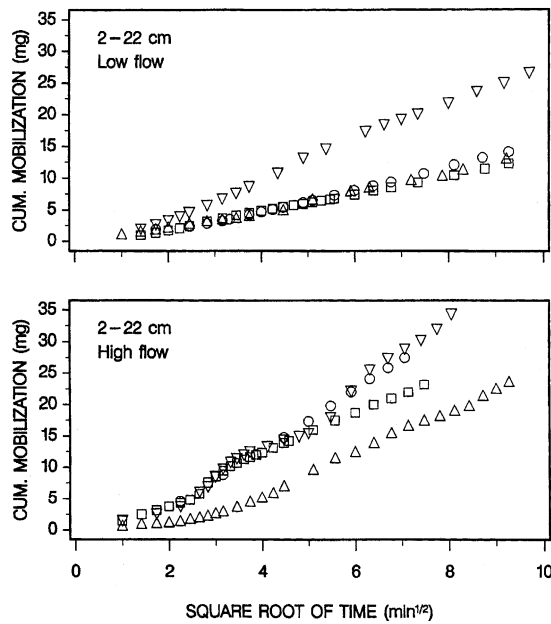


Fig. 5. Cumulative colloid mobilization as a function of the square root of time during leaching through intact macroporous soil cores. The linear relationship between these variables suggests that the kinetics of colloid mobilization were controlled by diffusion (from Jacobsen et al., 1997).

is based on the assumptions that mineral colloids are only mobilized at the soil surface, not within the soil profile, and that colloid deposition in both porewater domains can be described by simple first-order kinetics expressions. Calculations of the model of Jarvis et al. (1999) agree reasonably well with colloid concentrations measured over an 80-d period in soil water samples collected from a tile-drained silty clay soil in Sweden.

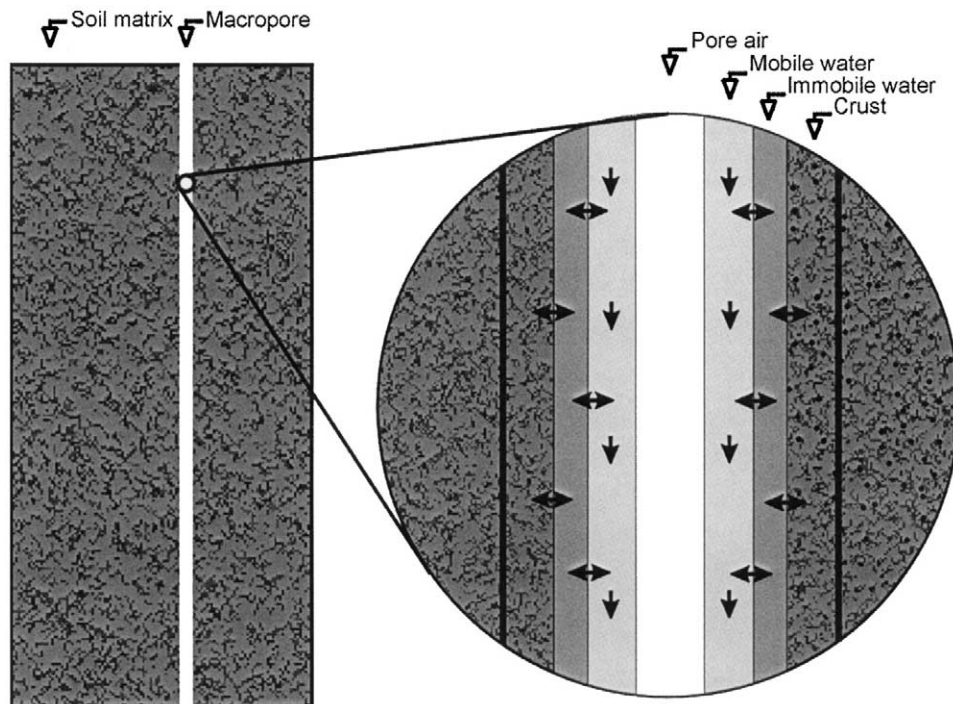


Fig. 6. Representation of a single equivalent macropore with colloid mass transfer between three phases: mobile water, immobile water, and crust. The horizontal arrows indicate colloid diffusion between phases, and the vertical arrows indicate advective colloid transport (from Schelde et al., 2002).

While progress has been made toward developing a capability to simulate the unsaturated transport of colloids in nonideal systems characterized by porous-medium heterogeneity, there is clearly a long way to go. Available models are very simple and incorporate only a subset of the mass-transfer processes that combine to influence colloid mobility in the vadose zone. Additional testing of models over a broader range of experimental conditions is needed. These model-data evaluations will lead to model refinement by illuminating gaps in our understanding of processes and will help to define quantitative relationships between model parameters and measurable system properties.

## FUTURE DIRECTIONS

To better understand colloid movement through the unsaturated zone, five major areas of research should be emphasized: (i) improved visualization of unsaturated flow and colloid transport phenomena, (ii) continued investigation of transient flow (wetting and drying) conditions, (iii) further examination of the effects of soil structure on colloid mobilization and transport, (iv) better quantification of pore straining of colloids and its effect of soil clogging, and (v) assessment of colloid mobilization under extreme conditions present at waste sites.

Using tools like light transmission through transparent micro- and meso-models (Wan and Wilson, 1994a; Sirivithayapakorn and Keller, 2003), magnetic resonance imaging, and X-ray computed tomography, efforts are underway to improve our understanding of flow and colloid transport in the unsaturated zone (Darnault et al., 2002; Nestle et al., 2002; Wildenschild et al., 2002; Weisbrod et al., 2003). As the resolution and capabilities of these visualization systems improve, it will be possible to test hypotheses regarding proposed mechanisms of colloid mobilization and deposition, as well as to identify new mechanisms that cannot readily be inferred from analysis of column experiments. Visualization experiments



that permit air–water interface reactions to be unambiguously distinguished from solid–water interface reactions should be particularly useful in guiding the development of mechanistic models for colloid deposition and mobilization.

Transients in flow conditions—the wetting and drying cycles of soils—have recently been identified in field and laboratory experiments as key factors governing the mobilization of soil colloids (El-Farhan et al., 2000; Saiers and Lenhart, 2003b; Saiers et al., 2003). This transient flow–induced mobilization is particularly complex because it is governed by multiple mechanisms, including (but not limited to) thin-film expansion, air–water interface scour, and fluid shear. Additional field and laboratory studies on bulk soils, combined with better visualization techniques, are needed to evaluate the responses of these mechanisms for the range of physical and chemical conditions encountered in real vadose-zone environments. These observations are required to advance theory appropriate for quantifying colloid mobilization in near-surface soils, where transient-flow regimes predominate.

Soil structure (i.e., preferential flow paths, aggregates) plays an important role in infiltration processes and thus in the mobilization and transport of colloid-sized particles. Disintegration of soil aggregates leads to the release of clay particles. Although observations of this phenomenon are available (Rengasamy et al., 1984; Pojasok and Kay, 1990; Brubaker et al., 1992; Oades, 1993; Le Bissonnais, 1996), additional research is needed to examine the relationship between colloid dispersion in the typical batch system and in intact soils. A recent step in this direction is the work of Kjaergaard et al. (in press), who observed a correlation between the amount of clay released from soils taken from a hill slope sequence with a wide range of clay content and the amount of clay released by a “low-energy” water-dispersible colloid batch experiment. Their low-energy test used soils at field moisture contents and less vigorous shaking. Experiments with intact cores suggest that preferential flow paths (e.g., macropores) affect colloid transport and filtration (Jacobsen et al., 1997; Ryan et al., 1998; Lægdsmand et al., 1999; Schelde et al., 2002), but evaluating these processes in laboratory experiments with the goal of defining mechanisms is difficult. One of the fundamental issues that remain unresolved is identification of the conditions under which macropore flow is initiated, a problem common to all aspects of flow and transport in the vadose zone. To improve our understanding of the influences of preferential flow paths on colloid transport, we must better characterize the nature of these flow paths in natural soils and develop ways of reproducing them in model soil systems.

The effects of pore straining on the removal of larger colloids in saturated porous media is receiving renewed attention owing to concern about the transport of protozoan cysts during riverbank filtration (Bradford et al., 2002, 2003). The removal of colloids by film straining has been incorporated into models of colloid transport in the vadose zone, but pore straining has not. Pore straining of colloids will strongly affect soil permeability and may lead to irreversible clogging, an important concern for wastewater reclamation and soil aquifer treatment.

The importance of transients in porewater chemistry more drastic than the infiltration of rainwater of low ionic strength must also be evaluated. To assess colloid-facilitated contaminant migration at sites of improper disposal of hazardous and radioactive waste, we must examine colloid transport and mass-transfer processes at a broad range of porewater pH, porewater compositions, and temperatures (e.g., Gschwend et al., 1990; Flury et al., 2002; Blume et al., 2002). In addition, the formation of porewater colloids by precipitation of super-saturated mineral phases, which has been observed in both surface and groundwaters (e.g., Gschwend and Reynolds,

1987; Liang et al., 1993; Schemel et al., 2000), must be assessed in vadose zones subject to these hazardous-waste environments.

## ACKNOWLEDGMENTS

This work was supported by National Science Foundation grants EAR-9909553 (JNR) and EAR-9909508 (JES) and Department of Energy grants DE-FG07-02ER63492 (JES) and DE-FG07-02ER63491 (JNR).

## REFERENCES

- Abdel-Fattah, A.I., and M.S. El-Genk. 1998. Sorption of hydrophobic, negatively charged microspheres onto a stagnant air/water interface. *J. Colloid Interface Sci.* 202:417–429.
- Amrhein, C., P.A. Mosher, and J.E. Strong. 1993. Colloid-assisted transport of trace metals in roadside soils receiving deicing salts. *Soil Sci. Soc. Am. J.* 57:1212–1217.
- Baveye, P., P. Vandevivere, B.L. Hoyle, P.C. DeLeo, and D.S. de Lozada. 1998. Environmental impact and mechanisms of biological clogging of saturated soils and aquifer materials. *Crit. Rev. Environ. Sci. Technol.* 28:123–191.
- Beven, K., and P. Germann. 1982. Macropores and water flow in soils. *Water Resour. Res.* 18:1311–1325.
- Bhattacharjee, S., C.-H. Ko, and M. Elimelech. 1998. DLVO interaction between rough surfaces. *Langmuir* 14:3365–3375.
- Biddle, D.L., D.J. Chittleborough, and R.W. Fitzpatrick. 1995. Field monitoring of solute and colloid mobility in a gneissic sub-catchment, South Australia. *Appl. Clay Sci.* 9:433–442.
- Blume, T., N. Weisbrod, and J.S. Selker. 2002. Permeability changes in layered sediments: Impacts of particle release. *Ground Water* 40:466–474.
- Bond, W.J. 1986. Illuvial band formation in a laboratory column of sand. *Soil Sci. Soc. Am. J.* 50:265–267.
- Bradford, S.A., S.R. Yates, M. Bettahar, and J. Simunek. 2002. Physical factors affecting the fate and transport of colloid in saturated porous media. *Water Resour. Res.* 38:1327. doi: 10.1029/2002WR001240.
- Bradford, S.A., J. Simunek, M. Bettahar, M.Th. van Genuchten, and S.R. Yates. 2003. Modeling colloid attachment, straining, and exclusion in saturated porous media. *Environ. Sci. Technol.* 37:2242–2250.
- Brubaker, S.C., C.S. Holzhey, and B.R. Brasher. 1992. Estimating the water-dispersible clay contents of soils. *Soil Sci. Soc. Am. J.* 56:1227–1232.
- Buol, S.W., and F.D. Hole. 1961. Clay skin genesis in Wisconsin soils. *Soil Sci. Soc. Am. Proc.* 25:377–379.
- Cherrey, K.D., M. Flury, and J.B. Harsh. 2003. Nitrate and colloid transport through coarse Hanford sediments under steady state, variably saturated flow. *Water Resour. Res.* 39:1165. doi: 10.1029/2002WR001944.
- Chu, Y., Y. Jin, M. Flury, and M.V. Yates. 2001. Mechanisms of virus removal during transport in unsaturated porous media. *Water Resour. Res.* 37:253–263.
- Coats, K., and B. Smith. 1964. Dead-end pore volume and dispersion in porous media. *SPE J.* 4:73–84.
- Corapcioglu, M.Y., and H. Choi. 1996. Modeling colloid transport in unsaturated porous media and validation with laboratory column data. *Water Resour. Res.* 32:3437–3449.
- Crank, J. 1975. *The mathematics of diffusion.* Oxford University Press, Oxford, UK.
- Darnault, C.J.G., D.A. DiCarlo, T.W.J. Bauters, T.S. Steenhuis, J.-Y. Parlange, C.D. Montemagno, and P. Baveye. 2002. Visualization and measurement of multiphase flow in porous media. *Ann. N. Y. Acad. Sci.* 972:103–110.
- de Jonge, H., O.H. Jacobsen, L.W. de Jonge, and P. Moldrup. 1998. Particle-facilitated transport of prochloraz in undisturbed sandy loam soil columns. *Soil Sci. Soc. Am. J.* 27:1495–1503.
- Derjaguin, B.V., and L. Landau. 1941. Theory of the stability of strongly charged lyophobic sols and of the adhesion of strongly charged particles in solutions of electrolytes. *Acta Physicochim. URSS* 14:633–662.
- El-Farhan, Y.H., N.M. DeNovio, J.S. Herman, and G.M. Hornberger. 2000. Mobilization and transport of soil particles during infiltration

- experiments in an agricultural field, Shenandoah Valley, Virginia. *Environ. Sci. Technol.* 34:3555–3559.
- Elimelech, M., J. Gregory, X. Jia, and R. Williams. 1995. Particle deposition and aggregation. Butterworth-Heinemann Ltd., Oxford, UK.
- Flury, M., J.B. Mathison, and J.B. Harsh. 2002. In situ mobilization of colloids and transport of cesium in Hanford sediments. *Environ. Sci. Technol.* 36:5335–5351.
- Frenkel, H., J.O. Goertzen, and J.D. Rhoades. 1978. Effects of clay type and content, exchangeable sodium percentage, and electrolyte concentration on clay dispersion and soil hydraulic conductivity. *Soil Sci. Soc. Am. J.* 42:32–39.
- Gamerding, A.P., and D.I. Kaplan. 2001. Physical and chemical determinants of colloid transport and deposition in water-unsaturated sand and Yucca Mountain tuff material. *Environ. Sci. Technol.* 35:2497–2504.
- Gomez-Suarez, C., H.J. Busscher, and H.C. van der Mei. 2001. Analysis of bacterial attachment from substratum surfaces by the passage of air-liquid interfaces. *Appl. Environ. Microbiol.* 67:2531–2537.
- Gomez-Suarez, C., J. Noordmans, H.C. van der Mei, and H.J. Busscher. 1999. Removal of colloidal particles from quartz collector surfaces as stimulated by the passage of liquid-air interfaces. *Langmuir* 15:5123–5127.
- Grolimund, D., and M. Borkovec. 1999. Long-term release kinetics of colloidal particles from natural porous media. *Environ. Sci. Technol.* 33:4054–4060.
- Grout, H., A.M. Tarquis, and M.R. Wiesner. 1998. Multifractal analysis of particle size distributions in soil. *Environ. Sci. Technol.* 32:1176–1182.
- Gschwend, P.M., D.A. Backhus, J.K. MacFarlane, and A.L. Page. 1990. Mobilization of colloids in groundwater due to infiltration of water at a coal ash disposal site. *J. Contam. Hydrol.* 6:307–320.
- Gschwend, P.M., and M.D. Reynolds. 1987. Monodisperse ferrous phosphate colloids in an anoxic groundwater plume. *J. Contam. Hydrol.* 1:309–327.
- Hahn, M., and C.R. O'Melia. 2004. Deposition and reentrainment of Brownian particles in porous media under unfavorable chemical conditions: Some concepts and applications. *Environ. Sci. Technol.* 38:210–220.
- Harris, W.G., V.W. Carlisle, and S.L. Chesser. 1987. Clay mineralogy as related to morphology of Florida soils with sandy epipedons. *Soil Sci. Soc. Am. J.* 51:1673–1677.
- Herzig, J.P., D.M. Leclerc, and P. Le Goff. 1970. Flow of suspensions through porous media—Application to deep filtration. *Ind. Eng. Chem.* 62:8–35.
- Hubbe, M.A. 1985. Detachment of colloidal hydrous oxide spheres from flat solids exposed to flow. 2. Mechanism of release. *Colloids Surf.* 16:249–270.
- Hurst, C.J. 1980. Survival of enteroviruses in rapid-infiltration basins during the land application of waste-water. *Appl. Environ. Microbiol.* 40:192–200.
- Jacobsen, O.H., P. Moldrup, C. Larsen, L. Konnerup, and L.W. Petersen. 1997. Particle transport in macropores of undisturbed soil columns. *J. Hydrol.* 196:185–203.
- Jarvis, N.J., K.G. Villholth, and B. Ulen. 1999. Modeling particle mobilization and leaching in macroporous soil. *Eur. J. Soil Sci.* 50:621–632.
- Jewett, D.G., B.E. Logan, R.G. Arnold, and R.C. Bales. 1999. Transport of *Pseudomonas fluorescens* strain P17 through quartz sand columns as a function of water content. *J. Contam. Hydrol.* 36: 73–89.
- Kaplan, D.I., P.M. Bertsch, and D.C. Adriano. 1997. Mineralogical and physicochemical differences between mobile and nonmobile colloidal phases in reconstructed pedons. *Soil Sci. Soc. Am. J.* 61:641–649.
- Kaplan, D.I., P.M. Bertsch, D.C. Adriano, and W.P. Miller. 1993. Soil-borne mobile colloids as influenced by water flow and organic carbon. *Environ. Sci. Technol.* 27:1193–1200.
- Kjaergaard, C., L.W. de Jonge, P. Moldrup, and P. Schjonning. 2004. Water-dispersible colloids: Effects of measurement method, clay content, initial soil matric potential, and wetting rate. Available at [www.vadosezonejournal.org](http://www.vadosezonejournal.org). *Vadose Zone J.* 3:403–412 (this issue).
- Ko, C.-H., and M. Elimelech. 2000. The “shadow effect” in colloid transport and deposition in granular porous media: Measurements and mechanisms. *Environ. Sci. Technol.* 34:3681–3689.
- Lægdsmand, M., K.G. Villholth, M. Ullum, and K.H. Jensen. 1999. Processes of colloid mobilization and transport in macroporous soil monoliths. *Geoderma* 93:33–59.
- Le Bissonnais, Y. 1996. Aggregate stability and assessment of soil crustability and erodibility: I. Theory and methodology. *Eur. J. Soil Sci.* 47:425–437.
- Lenhart, J.J., and J.E. Saiers. 2002. Transport of silica colloids through unsaturated porous media: Experimental results and model comparisons. *Environ. Sci. Technol.* 36:769–777.
- Liang, L., J.F. McCarthy, L.W. Jolley, J.A. McNabb, and T.L. Melhorn. 1993. Iron dynamics: Transformation of Fe(II)/Fe(III) during injection of natural organic matter in a sandy aquifer. *Geochim. Cosmochim. Acta* 57:1987–1999.
- Logan, B.E., D.G. Jewett, R.G. Arnold, E.J. Bower, and C.R. O'Melia. 1995. Clarification of clean-bed filtration models. *J. Environ. Eng.* 121:869–873.
- Matlack, K.S., and D.W. Houseknecht. 1989. Emplacement of clay into sand by infiltration. *J. Sediment. Petrol.* 59:77–87.
- McDowell-Boyer, L.M. 1992. Chemical mobilization of micron-sized particles in saturated porous media under steady flow conditions. *Environ. Sci. Technol.* 26:586–593.
- McDowell-Boyer, L.M., J.R. Hunt, and N. Sitar. 1986. Particle transport through porous media. *Water Resour. Res.* 22:1901–1921.
- McGechan, M.B., and D.R. Lewis. 2002. Transport of particulate and colloid-sorbed contaminants through soil. Part 1: General principles. *Biosyst. Eng.* 83:255–273.
- McKeague, J.A., and R.J. St. Arnaud. 1969. Pedotranslocation: Eluviation-illuviation in soils during the Quaternary. *Soil Sci.* 107:428–434.
- Nestle, N., T. Baumann, and R. Niessner. 2002. Magnetic resonance imaging in environmental science. *Environ. Sci. Technol.* 36:154A–160A.
- Nkedi-Kizza, P., J.W. Biggar, H.M. Selim, M.Th. van Genuchten, P.J. Wierenga, J.M. Davidson, and D.R. Nielsen. 1984. On the equivalence of two conceptual models for describing ion exchange during transport through an aggregated oxisol. *Water Resour. Res.* 20:1123–1130.
- Noack, A.G., C.D. Grant, and D.J. Chittleborough. 2000. Colloid movement through stable soils of low cation-exchange capacity. *Environ. Sci. Technol.* 34:2490–2497.
- Oades, J.M. 1993. The role of biology in the formation, stabilization and degradation of soil structure. *Geoderma* 56:377–400.
- O'Neill, M.E. 1968. A sphere in contact with a plane wall in a slow linear shear flow. *Chem. Eng. Sci.* 23:1293–1298.
- Pilgrim, D.H., and D.D. Huff. 1983. Suspended sediment in rapid subsurface stormflow on a large field plot. *Earth Surf. Proc. Landforms* 8:451–463.
- Pojasok, T., and B.D. Kay. 1990. Assessment of a combination of wet sieving and turbidimetry to characterize the structural stability of moist aggregates. *Can. J. Soil Sci.* 70:33–42.
- Posadas, A.N.D., D. Giménez, M. Bittelli, C.M.P. Vaz, and M. Flury. 2001. Multifractal characterization of soil particle-size distributions. *Soil Sci. Soc. Am. J.* 65:1361–1367.
- Powelson, D.K., C.P. Gerba, and M.T. Yahya. 1993. Virus transport and removal in waste-water during aquifer recharge. *Water Res.* 27:583–590.
- Quirk, J.P., and R.K. Schofield. 1955. The effect of electrolyte concentration on soil permeability. *J. Soil Sci.* 6:163–178.
- Rajagopalan, R., and C. Tien. 1976. Trajectory analysis of deep-bed filtration with the sphere-in-cell porous media model. *AIChE J.* 22:523–533.
- Redman, J.A., S.B. Grant, T.M. Olson, and M.K. Estes. 2001. Pathogen filtration, heterogeneity, and potable reuse of wastewater. *Environ. Sci. Technol.* 35:1798–1805.
- Rengasamy, P., R.S.B. Greene, and G.W. Ford. 1984. The role of clay fraction in the particle arrangement and stability of soil aggregates: A review. *Clay Res.* 3:53–67.
- Ryan, J.N., and M. Elimelech. 1996. Colloid mobilization and transport in groundwater. *Colloids Surf. A* 107:1–56.
- Ryan, J.N., and P.M. Gschwend. 1994. Effect of ionic strength and flow rate on colloid release: Relating kinetics to intersurface potential energy. *J. Colloid Interface Sci.* 164:21–34.

- Ryan, J.N., T.H. Illangasekare, M.I. Litaor, and R. Shannon. 1998. Particle and plutonium mobilization in macroporous soils during rainfall simulations. *Environ. Sci. Technol.* 32:476–482.
- Saiers, J.E., G.M. Hornberger, D.B. Gower, and J.S. Herman. 2003. The role of moving air–water interfaces in colloid mobilization within the vadose zone. *Geophys. Res. Lett.* 30:2083. doi:10.1029/2003GL018418.
- Saiers, J.E., and J.J. Lenhart. 2003a. Ionic-strength effects on colloid transport and interfacial reactions in partially saturated porous media. *Water Resour. Res.* 39:1256. doi:10.1029/2002WR001887.
- Saiers, J.E., and J.J. Lenhart. 2003b. Colloid mobilization and transport within unsaturated porous media under transient-flow conditions. *Water Resour. Res.* 39:1019. doi:10.1029/2002WR001370.
- Sakthivadivel, R. 1966. Theory and mechanism of filtration of non-colloidal fines through a porous medium. Rep. HEL 15-5. Hydraulic Engineering Laboratory, University of California, Berkeley.
- Schäfer, A., P. Ustohal, H. Harms, F. Stauffer, T. Dracos, and A.J.B. Zehnder. 1998. Transport of bacteria in unsaturated porous media. *J. Contam. Hydrol.* 33:149–169.
- Schelde, K., P. Moldrup, O.H. Jacobsen, H. de Jonge, L.W. de Jonge, and T. Komatsu. 2002. Diffusion-limited mobilization and transport of natural colloids in macroporous soil. Available at www.vadosezonejournal.org. *Vadose Zone J.* 1:125–136.
- Schemel, L.E., B.A. Kimball, and K.E. Bencala. 2000. Colloid formation and metal transport through two mixing zones affected by acid mine drainage near Silverton, Colorado. *Appl. Geochem.* 15: 1003–1018.
- Selker, J.S., C.K. Keller, and J.T. McCord. 1999. *Vadose zone processes*. Lewis Publishers, Boca Raton, FL.
- Sim, Y., and C.V. Chrysikopoulos. 2000. Virus transport in unsaturated porous media. *Water Resour. Res.* 36:173–179.
- Sirivithayapakorn, S., and A. Keller. 2003. Transport of colloids in unsaturated porous media: A pore-scale observation of processes during the dissolution of the air–water interface. *Water Resour. Res.* 39:1346. doi:10.1029/2003WR002487.
- Tarback, E.J., and F.K. Lutgens. 1997. *Earth: An introduction to physical geology*. 3rd ed. Prentice Hall, Englewood Cliffs, NJ.
- Tufenkji, N., and M. Elimelech. 2004. Correlation equation for predicting single-collector efficiency in physicochemical filtration in saturated porous media. *Environ. Sci. Technol.* 38:529–536.
- van Genuchten, M.Th., and R. Cleary. 1979. Movement of solutes in soil: Computer-simulated and laboratory results. p. 349–386. In G.H. Bolt (ed.) *Soil chemistry. B. Physicochemical models*. Elsevier, Amsterdam.
- Verwey, E.J.W., and J.T.G. Overbeek. 1948. *Theory of the stability of lyophobic colloids*. Elsevier, Amsterdam.
- Wan, J., and T.K. Tokunaga. 1997. Film straining of colloids in unsaturated porous media: Conceptual model and experimental testing. *Environ. Sci. Technol.* 31:2413–2420.
- Wan, J., and T.K. Tokunaga. 2002. Partitioning of clay colloids at air–water interfaces. *J. Colloid Interface Sci.* 247:54–61.
- Wan, J., and J.L. Wilson. 1994a. Visualization of the role of the gas–water interface on the fate and transport of colloids in porous media. *Water Resour. Res.* 30:11–23.
- Wan, J., and J.L. Wilson. 1994b. Colloid transport in unsaturated porous media. *Water Resour. Res.* 30:857–864.
- Weisbrod, N., O. Dahan, and E.M. Adar. 2002. Particle transport in unsaturated fractured chalk under arid conditions. *J. Contam. Hydrol.* 56:117–136.
- Weisbrod, N., M.R. Niemet, and J.S. Selker. 2003. Light transmission technique for the evaluation of colloidal transport and dynamics in porous media. *Environ. Sci. Technol.* 37:3694–3700.
- Wildenschild, D., J.W. Hopmans, C.M.P. Vaz, M.L. Rivers, D. Rikard, and B.S.B. Christensen. 2002. Using X-ray computed tomography in hydrology: Systems, resolutions, and limitations. *J. Hydrol.* 267: 285–297.
- Wu, Q., M. Borkovec, and H. Sticher. 1993. On particle-size distribution in soils. *Soil Sci. Soc. Am. J.* 57:883–890.
- Yao, K.M., M.T. Habibian, and C.R. O’Melia. 1971. *Water and waste water filtration: Concepts and applications*. *Environ. Sci. Technol.* 5:1105–1112.